Research Article

The effect of physicochemical properties on paracetamol photodegradation in cuboid bubble column

Ashwan HAMAD KHALİL, **Asawer ALWASİTİ**[*], **Jenan ABDULRZAAK**, **Abbas AL-SHALAL**

Department of Chemical Engineering, University of Technology, Baghdad, Iraq

ABSTRACT

Paracetamol is one of the most anthropogenic micropollutants, and their removal from the environment often requires a specialized method of remediation. In this study, a photocatalyst technique aided with air bubbles was used to degrade the pharmaceutical pollutant paracetamol (PCT) from the water via the COD test and HPLC analysis under different operating conditions. The experiments were carried out in a semi-batch rectangular bubble column with dimensions of 1500 mm height, 30 mm depth, and 200 mm width under UV light. Titanium oxide (TiO_2) was used as a source of catalyst. The effect of operating conditions of pH (3–10), air flow rate (0–2) L/min, salinity of solution represented by NaCl concentration (0–1000) mg/L, and 240 min irradiation time on the paracetamol removal were studied. The Box–Behnken design was adopted to study the individual effects of pH (A), air flow rate (B), and salinity (C) and their interactive effects. From the experimental and regression data, a second-order polynomial regression model is predicted, and the variance analysis of the regressions shows that the linear terms (A and B), and all quadratic terms (A, B, and C) have significant effects on the removal percentage of COD. According to numerical optimization, the greatest %COD removal is 76.7 in the process conditions of 5.3 pH, 1L/min, and 269 mg/L of NaCl. The experimental results show that the maximum %COD removal was 78% at pH=7, 1L/min, and 0mg/L of NaCl. HPLC analysis shows 91.2% of paracetamol degradation.

Cite this article as: Hamad Khalil A, Alwasiti A, Abdulrzaak J, Al-Shalal A. The effect of physicochemical properties on paracetamol photodegradation in cuboid bubble column. Environ Res Tec 2023;6(4)347–358.

INTRODUCTION

Due to the increase in the world's human population and industrial development, water pollution has been an alarming issue globally. The pollutants in the water come from the effluent of industries (e.g., the textile industry, paper industry, the pharmaceutical industry, etc.) and domestic pollutants (e.g., pharmaceuticals, pesticides, detergents, etc.) [1, 2]. Pharmaceutical pollutants can be considered among the pollutants that are largely present in wastewater due to the diversity of their sources, whether they are from factories or household pollutants. Due to its high value and low volume in wastewater, it has become the focus of researchers' attention. Since 2000, many researchers [3–6] published research demonstrating the prevalence of pharmaceuticals in aquatic habitats. This has sparked significant issues about the lack of understanding about the possible consequences of pharmaceutical chemicals and their metabolites on human and aquatic creatures, even though they exist in little trace amounts [7, 8]. One of the widely used pharmaceutical drugs is paracetamol (commonly known as acetaminophen) [9–12]. Parac-

etamol residues and metabolites have been found in waterbodies all over the world [13, 14]. At therapeutic doses, paracetamol is safe; but, at higher concentrations, it may undergo an oxidative transition to N-acetyl-p-benzoquinone imine (NAPQI) [15]. This toxic chemical causes liver necrosis as well as an uncommon skin condition [16]. On therapeutic usage, around 58–68% of paracetamol and its metabolite are eliminated from the body [17]. These percentages are discharged into the water in general, which leads to pollution.

In recent years, new technologies for paracetamol degradation in wastewater have been developed, like electrocoagulation [18], non-thermal Plasma [19], ozonation and H_2O_2/ UV system [20–22], chlorination treatment [23], and Fenton process [24]. Among those processes, the chemical process that deals with photocatalysts such as TiO_2, ZnO, etc. can dismantle the industrial wastewater [25].

Heterogeneous photocatalysis with titanium photocatalyst is a rapidly growing technology for removing refractory and toxic organic pollutants from water, such as dyes, pesticides, petroleum contaminates and pharmaceuticals [26–32] The efficacy of these environmentally friendly photochemical wastewater treatment technologies is related to the in situ creation of aggressively oxidizing hydroxyl radicals ($\cdot$OH), which oxidize a wide spectrum of organic contaminants found in water and wastewaters [33, 34].

Titanium dioxide is one of the most promising semiconductors for photocatalytic pollution removal since various organic compounds may be reduced to tiny pieces or mineralized in water at room temperature and pressure [35, 36]. The following reactions have been identified as occurring when TiO_2 interacts with light [37]:

$$TiO_2 + h\nu \rightarrow e_{CB}^- + h_{VB}^+ \tag{1}$$

$$e_{CB}^- + O_2 + H^+ \rightarrow HO_2^{\cdot} \tag{2}$$

$$e_{CB}^- + HO_2^{\cdot} + H^+ \rightarrow H_2O_2 \tag{3}$$

$$2e_{CB}^- + O_2 + 2H^+ \rightarrow H_2O_2 \tag{4}$$

$$h_{VB}^+ + H_2O \rightarrow HO^{\cdot} + H^+ \tag{5}$$

$$2HO^{\cdot} \rightarrow H_2O_2 \tag{6}$$

$$H_2O_2 + h\nu \rightarrow 2HO^{\cdot} \tag{7}$$

$$H_2O_2 + e_{CB}^- + H^+ \rightarrow HO^{\cdot} + H_2O \tag{8}$$

Several operational factors such as solution pH, metal loading, catalyst dose, starting concentration, light wavelength, and salinity influenced the photocatalytic destruction of the organic pollutants process [38]. According to published research [39, 40], the existence of inorganic salts can reduce or enhance photocatalytic efficacy depending on their composition, concentration, and solution pH. There has been no extensive research on saline wastewater with salinities ranging from 500 to 2,000 mg/L utilizing

photocatalytic oxidation techniques. Hence, such a study will be beneficial in giving the knowledge required for the treatment of saline wastewater. Although many researchers have examined the elimination of pharmaceutical waste using photocatalysts, the need to optimize this process is currently being investigated. As a result, unlike previous research, this work intends to increase process efficiency by employing air bubbles in a cuboid bubble column. Therefore, the novelty of the work is to investigate the effectiveness of air bubbles in the degradation of paracetamol in a UV-photo catalyst using a cuboid bubble column, where it was done at air flow rates (0–2) L/min and pH variables (3–10) and salinity (0–1000) mg/L through R.S.M. Their individual and interactive effects towards the COD removal and HPLC analysis are examined.

MATERIALS AND METHODS

Materials
The materials used for this experiment include: Titanium dioxide (TiO_2) (United States, Nanoparticles 10–30 nm Anatase), pharmaceutical (paracetamol, Samaraa SDI/Iraq), Hydrochloric acid (99% purity, AUSTRIA) and sodium hydroxide (98% purity, India) (to adjust the pH of the wastewater), and sodium chloride (India).

Experimental Methods
The photocatalytic process experiments were conducted by batch and semi-batch systems. The batch system is a 1liter beaker agitated by a magnetic stirrer (Shanghai, China, HS-12) In this process, titanium dioxide is added to the previously prepared solution (0.5 g/liter), and then it is irradiated by UV light for four hours. During this period, a sample is drawn every 1 hour. This process is repeated with different pH values (3, 7, 9) and for different salinity values. The samples that were withdrawn every 1 hour are collected and the chemical oxygen demand (COD) is measured.

The semi-batch system consists of a rectangular glass column (200 mm wide, 30 mm deep, 1500 mm high, and 6 mm thick). Air bubbles enter from the bottom of the column through a gas distributor, placed in the middle of the column bottom plate, which consists of 21 needles with a 5 mm square and 1mm inner diameter. The air is compressed using a gas compressor and a flow meter was used to control the flow rate, as shown in Figure 1. The bubble column was irradiated by a tube-type (60 cm length) UV-C lamp (T5 (G5), W=12 m^2, 220V sterilizer Philippines tube, wavelength 253.7 nm) carried by a sterile tube with a distance of 150 mm. The bubble column and the UV lamp were covered with aluminum foil to avoid the interference of UV light.

The wastewater solution was prepared by adding 300 mg of ground paracetamol in a beaker of 1 liter of distilled water and left on the stirrer for 5 minutes. Then 0.5 mg of TiO_2 is treated with distilled water using an ultrasonic device for 20 minutes. The homogenate mixture was added to the wastewater solution.
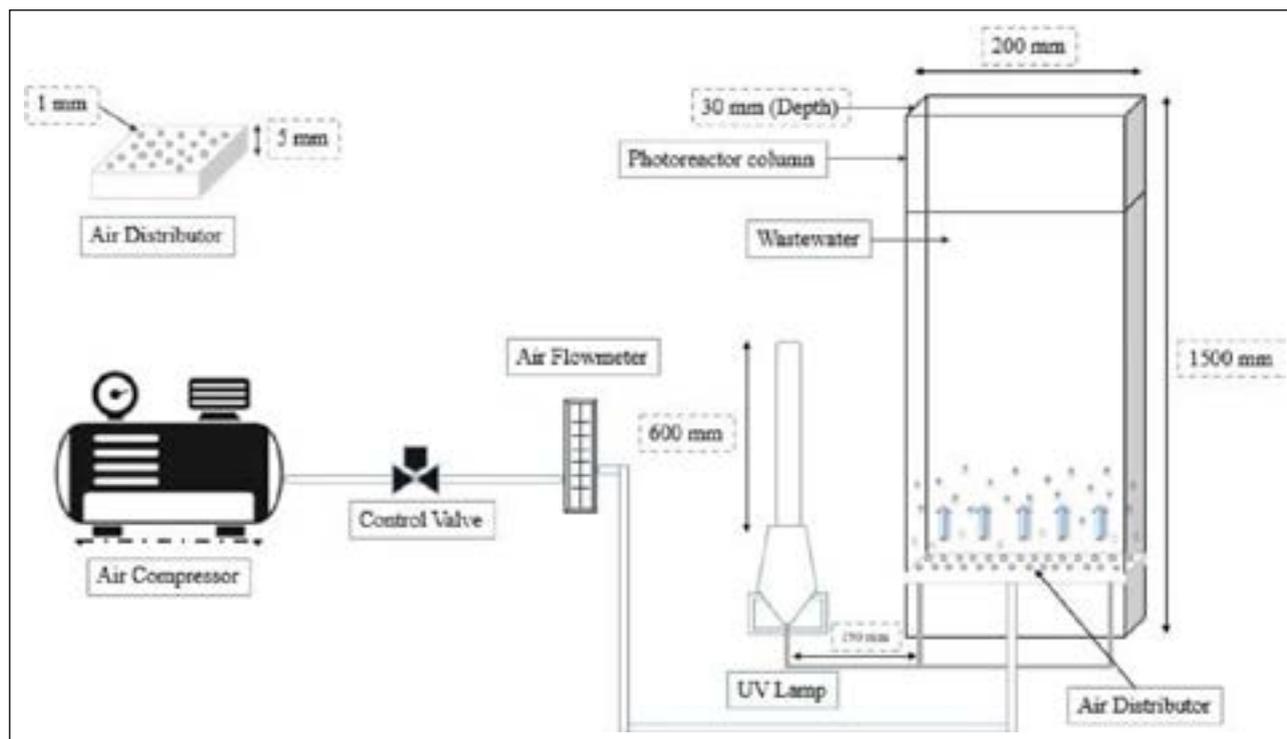
Figure 1. The schematic apparatus.

Table 1. The actual and coded values of the Box-Behnken design variables

	Factors	Coded and actual value		
		-1	0	+1
A	pH	3	7	10
B	Air Flow Rate, L/min	0	1	2
C	Salinity (NaCl concentration) mg/L	0	500	1000

The pH of the solution was changed to (3, 7, and 10) by adding HCl for the acidic medium and (NaOH) for the basic media. After, the solution was added to the bubble column and air bubbles were through in at rates of (1 and 2 L/min). The solution was exposed to ultraviolet radiation for (60, 120, 180, and 240) min. The effect of the salinity parameter was studied by adding two concentrations (500 and 1000) mg/L of sodium chloride to the prepared solution and reading the electrical conductivity of the two cases in the batch system and the semi-batch system.

The efficiency of the proposed removal method was investigated by measuring the chemical oxygen demand (COD) on samples for each irradiation time.

Experimental Design Parameters
The Box-Behnken method was employed in the statistical design of trials to investigate the individual and combined impacts of operational conditions (independent variables) on paracetamol degradation. The following steps were taken to complete the design: (i) experiment design utilizing a statistical model, (ii) response prediction, and (iii) building a mathematical

model, calculating the coefficients, and then examining the model's applicability. pH of the solution, concentration of salt, and airflow rate are the three independent variables considered. The independent variables were tested at 3–10, concentrations of 0–1000 mg/L, and 0–3 L/min, respectively. For the design of the experimental run (DoE) matrix, a Box Behnken method with three factors was employed with three levels. Table 1 shows the actual levels and coded levels of each component. There were 17 randomized experimental runs in all, including 12 factorial points and 5 center points. The removal efficiency of COD, after 240 minutes of photocatalytic reaction, was chosen as the response.

A second-order polynomial model to describe the response surface was obtained by multiple regression techniques using Design Expert software. The mathematical expression of the dependent variable (response) on the independent variables was equivalent to a quadratic polynomial.

$$R\% = +b_0 - b_1A + b_2B + b_3C + b_4AB + b_5AC + b_6BC + b_7A^2 + b_8B^2 + b_{10}C^2 \quad (9)$$

In which that R% is the removal efficiency of COD and (b_0-b_{10}) are variable coefficients.
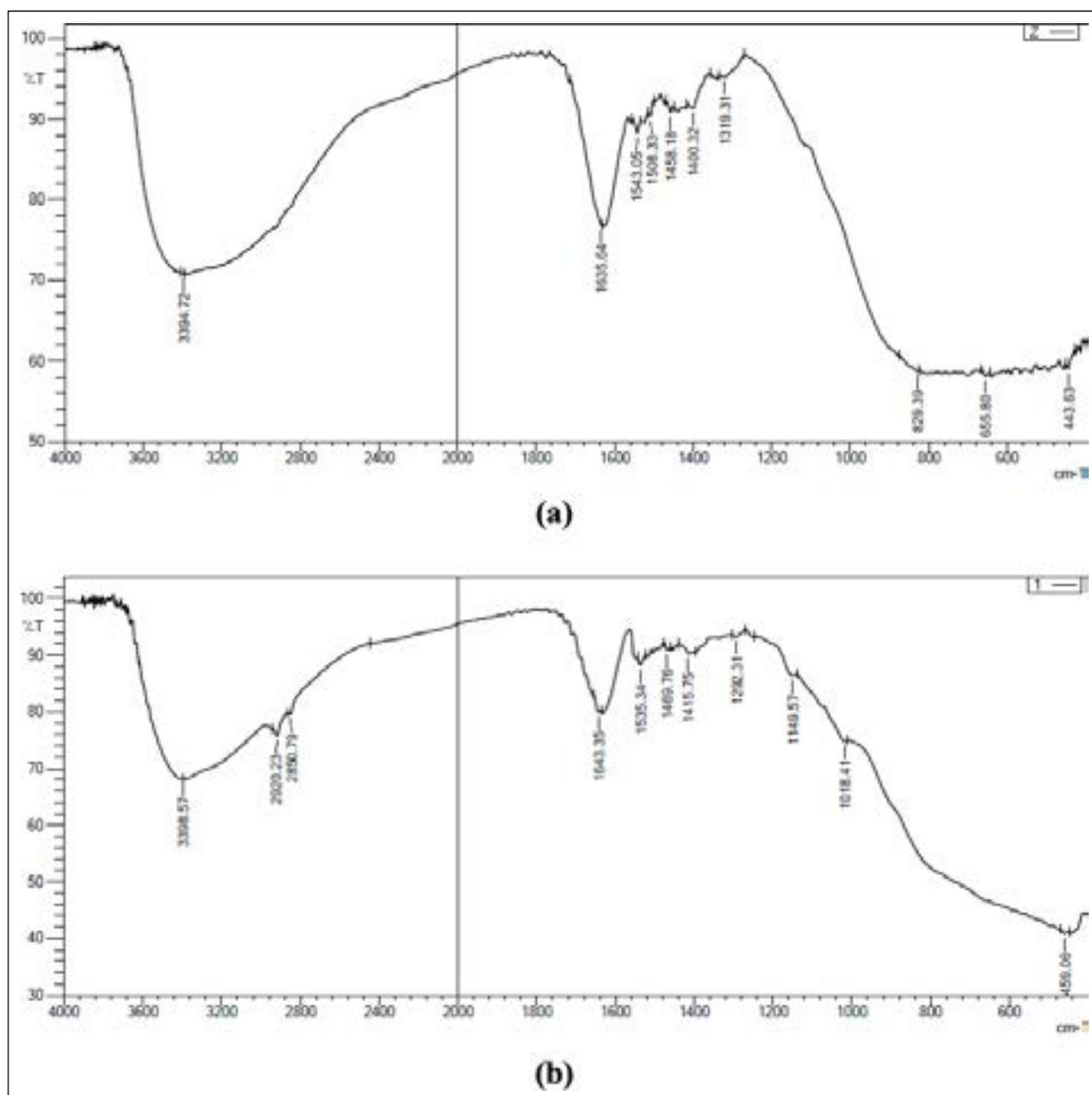
Figure 2. FTIR test of TiO_2, **(a)** before test, **(b)** after test (240 min).

RESULTS AND DISCUSSION

FTIR Characterization

FTIR is used to determine the functional groups and chemical structures of TiO_2 particles. As shown in Figures 2a, b, tests were carried out on TiO_2 powder before and after the photocatalytic process. The FTIR spectra were conducted in the 4000–400 cm^{-1} range.

In Figure 2a the broadband from 1000 to 400 cm^{-1} showed peaks (443.63, 655.80, 829.39) cm^{-1}. This region is ascribed to the Ti–O stretching and Ti–O–Ti bridging stretching mode and those peaks indicate that the powder is a mixture of anatase and rutile. After 240 minutes of work the FTIR test shows peaks (495.06 and 1018.41) cm^{-1}. This indicates that titanium is still effective after the photocatalyst

process. The spectra showed the peaks (1319.31 to 1543.05) cm^{-1} in Figure 2a indicating the presence of carboxyl (C=O) and methylene groups. Those peaks gradually decreased to (1292.31 to 1535.34) cm^{-1} after 4 hours of work as shown in Figure 2b. The peak at the (1635.64 cm^{-1}) in Figure 2a. is due to the amide group, this value lightly increased to 1643.35 cm^{-1} after the process, this is due to the degradation process of PMA that can result in some amide group. The peaks observed in Figure 2b, 2920.23 cm^{-1} and 2850.79 cm^{-1}, were due to the bending vibrations of the alkane (C–H) groups, which can appear during PMA degradation. Those peaks are not available in Figure 2a [28].

The peak observed at 3394.76 cm^{-1}, in Figure 2a is due to the stretching vibration of the O–H group, while in Figure 2b after 4 hours of photocatalyst process, the peaks identi-

Table 2. The Experimental run

Run	Factors						Response	
	pH		Air flow rate, L/min		NaCl concentration (mg/L)		%COD removal	
	Coded	Actual	Coded	Actual	Coded	Actual	Experimental	Predicted
1	-1	3	-1	0	0	500	38	43.55
2	0	7	0	1	0	500	76	76
3	+1	10	-1	0	0	500	13	16.89
4	+1	10	0	1	-1	0	26	25.7
5	0	7	-1	0	+1	1000	66	59.71
6	0	7	0	1	0	500	76	76
7	+1	10	0	1	+1	1000	27	30.3
8	-1	3	0	1	-1	0	54	51.15
9	0	7	-1	0	-1	0	55	51.85
10	0	7	0	1	0	500	76	76
11	0	7	+1	2	+1	1000	37	40.15
12	0	7	0	1	0	500	76	76
13	+1	10	+1	2	0	500	17	10.11
14	-1	3	0	1	+1	1000	46	45.85
15	0	7	0	1	0	500	76	76
16	0	7	+1	2	-1	0	41	47.29
17	-1	3	+1	2	0	500	27	24.45
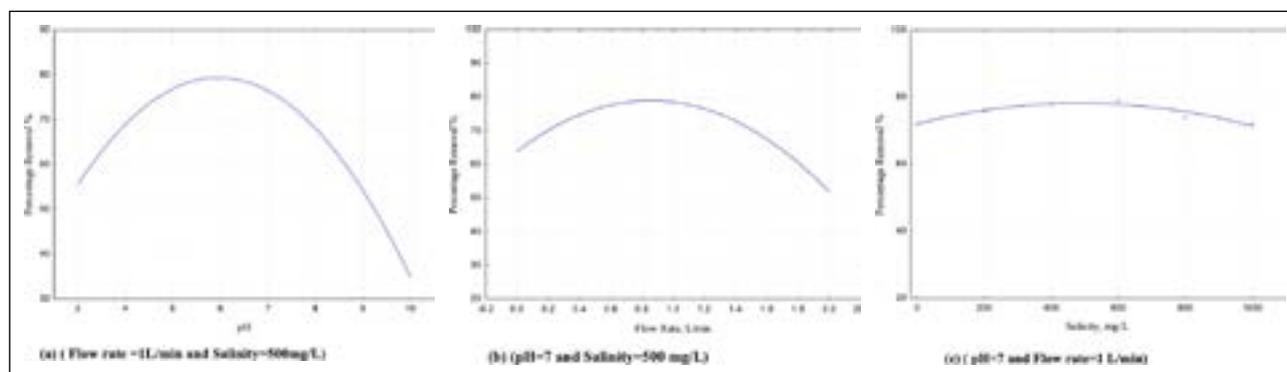
Figure 3. The 2D response surface plots.

fied at 3398.57 cm^{-1}, as shown in Figure 2b, indicating no change between them. Those peaks are the strong broad corresponding to the hydroxyl group's symmetric and asymmetric stretching vibrations due to water molecules. is related to the O–H stretching mode of the hydroxyl group, indicating the presence of moisture in the sample [34].

Response Surface Methodology
The impact of operational variables such as pH, salinity, and flow rate on photocatalytic paracetamol degradation was examined. To evaluate the individual and interaction impacts of these factors, a photocatalytic experimental design by CCD was used, followed by response surface analysis. Table 2 presents the experimental runs collected by Box-Behnken and the removal efficiency obtained in the experimental runs. The degradation effectiveness ranged from 18% to 76%.

The Response Surface Plots
The response surface plots of COD removal are shown in Figure 3. Figure 3a shows that increasing the pH and increasing the flow rate resulted in enhanced removal efficiency into the maximum point, after that the removal efficiency decreased. At acidic and alkaline pH, degradation efficiency is law, however, degradation efficiency increased at near-neutral pH.

The PZC condition is one in which the surface charge of TiO$_2$ is zero or neutral and its pH ranges from 4:5 to 7:0, depending on the catalysts used. TiO$_2$ used in this work, has a pH value at the isoelectric point approximately equal to 7, according to previous research [41].

The above results can be attributed to the effect of cations or anions in the solution, the paracetamol distribution, and
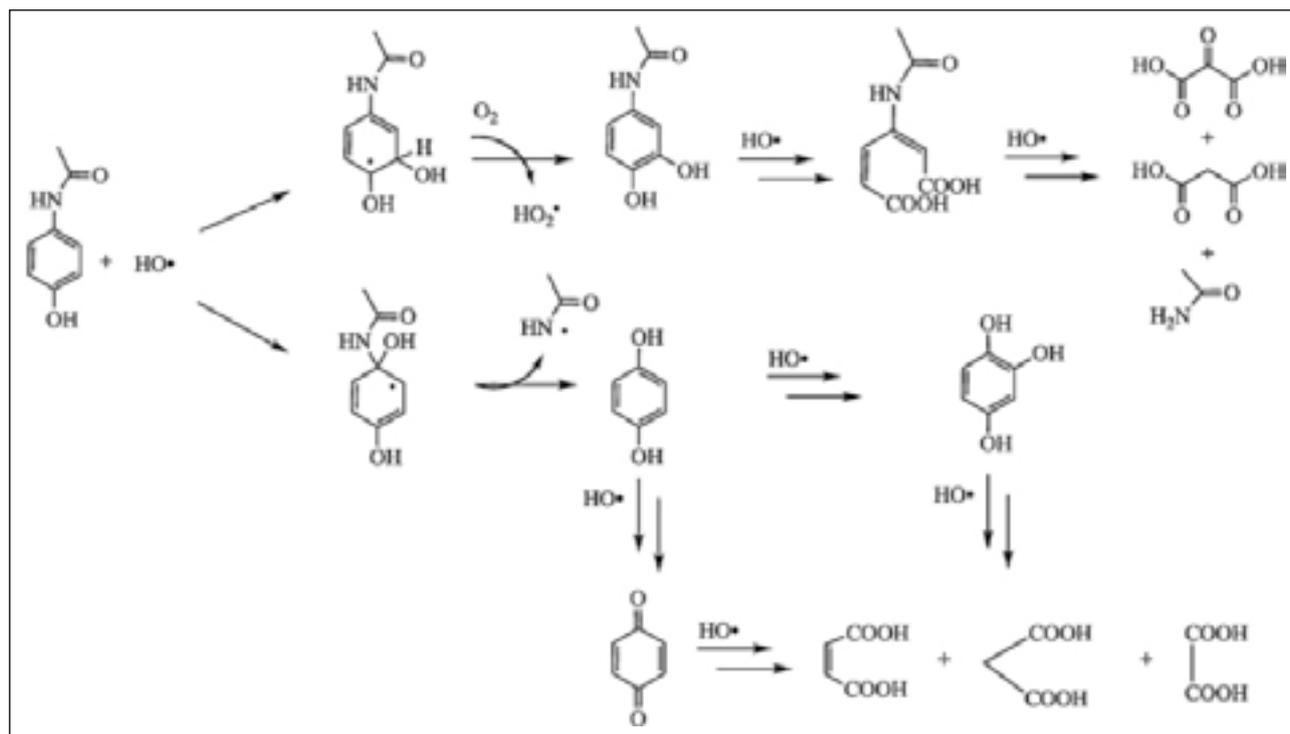
Figure 4. Paracetamol oxidation mechanism [43].

Table 3. The fit summary

Source	Sequential p-value	Std. Dev.	Adjusted R^2	Predicted R^2	
Linear	0.713	23.8	-0.112	-0.423	
2FI	0.982	26.91	-0.422	-1.637	
Quadratic	**<0.0001**	**5.58**	**0.938**	**0.572**	**Suggested**
Cubic		0	1		Aliased

the state of the TiO_2 surface according to the pH values on the photodegradation efficiency. Paracetamol tends to exist as anions in alkaline solutions (with higher pH values=9). Because of their high solubility in solution, such anions will not be considerably adsorbed. As a result, the electrostatic attraction between the TiO_2 surface (pHPZC=7) and paracetamol (pKa=10) increases [10], which is negatively charged at pH values, inhibiting paracetamol adsorption. As a result, paracetamol degrades more slowly in alkaline solutions. In acidic and natural solutions, paracetamol has a nonionic form and positively charged titanium dioxide causing low solubility in water, which increases adsorption on the TiO_2 surface and causes paracetamol breakdown. This result, however, disagrees with that obtained by [42], who determined that the optimal paracetamol degradation occurs at pH=9 and is not preferred to operate in acidic environments. This might be due to a variation in catalyst type as well as other operating circumstances.

The effect of the air bubbles on paracetamol degradation in the range of 0 to 2 L/min is shown in Figures 3b. The figures show that introducing air bubbles caused an increase in COD removal efficiency. The removal rate of COD at pH 7 was increased by 25% more than that using the batch pro-

cess at pH=7. The same effect of air bubbles is shown at pH =3 and pH=10, in which the COD removal efficiency was 54% and 26% respectively. The same trend is shown with different salinity concentrations of solution.

The impact of air bubbles may be explained by two factors. The first is that inserting air bubbles increases the molecules' diffusivity of paracetamol to the TiO_2 active sites owing to the turbulent flow, which increases the degradation rate. The second reason is that the airflow rate acts as a promoter by supplying the system with molecules of oxygen via the air bubbles. These oxygen molecules interact with the free electrons generated by UV light at the catalyst surface's active sites, Figure 4. According to the figure, the degradation of paracetamol during the photocatalytic process leads to the formation of byproducts at the beginning of the degradation, which are aromatic compounds, and at the end, carboxylic acids are formed. There are two most common paths for the degradation process, which are either getting rid of the –NH-CO-CH_3 group and then forming hydroquinone and 1,2,4-trihydroxy benzene and carboxylic acids, (2) or elimination of the CO-CH_3 group and then forming 4-aminophenol and 4-nitrophenol, before forming hydroquinone and 1,2,4-trihydroxy benzene and carboxyl-

Table 4. The ANOVA analysis of the quadratic model

Source	Sum of Squares	df	Mean Square	F-value	p-value	
Model	7929.86	9	881.1	28.29	0.0001	significant
A-pH	840.5	1	840.5	26.99	0.0013	
B-Flow Rate	331.51	1	331.51	10.64	0.0138	
C-Salinity	0.2475	1	0.2475	0.0079	0.9315	
AB	38.23	1	38.23	1.23	0.3045	
AC	24.75	1	24.75	0.7946	0.4023	
BC	56.25	1	56.25	1.81	0.2209	
A^2	4630.3	1	4630.3	148.66	<0.0001	
B^2	1747.96	1	1747.96	56.12	0.0001	
C^2	145.33	1	145.33	4.67	0.0676	
Residual	218.03	7	31.15			
Lack of Fit	218.03	3	72.68			
Pure Error	0	4	0			
Cor Total	8147.88	16				
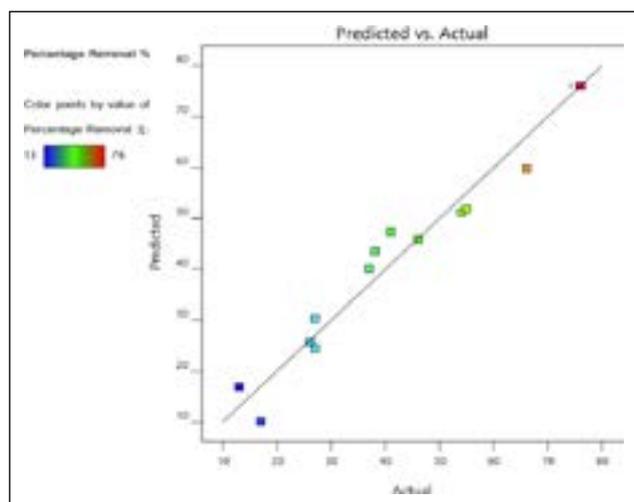
Figure 5. The experimental values vs. the predicted values.

ic acids. As a result of the suggested degradation process, more hydroxyl radicals are produced.

However, raising the flow rate to 2L/min reduces COD removal efficiency. This behavior may be linked to the increased flow rate, which causes the gas bubbles to merge, resulting in the development of huge bubbles and causing the bubble column to work in a heterogeneous pattern. The interaction between the nanoparticle and the UV will be reduced as a result of this heterogeneous pattern [43].

The effect of salinity is shown in Figure 3c. It is observed that there is little interaction effect between salinity, pH, and flow rate indicating salinity has little significant effect on the COD removal efficiency for all examined values of pH and air flow rate.

The prohibiting effect on the paracetamol degradation with the presence of some inorganic salts can be caused by several reasons [43–48]: (i) a decrease in light absorption by the photocatalyst caused by ions such as (Fe^{3+}), which act as an inner filter; (ii) an increase in recombination of h+ and e; (iii) the capturing of ($\cdot OH$) radicals or other oxidizing species; and (iv) adsorption competition with the reactant at the catalyst surface.

In this research NaCl was used as a source of salinity, the presence of Cl ions can cause many side reactions which can have positive and negative effects on paracetamol degradation. Chloride ions can be electrolyzed to produce chlorins, as shown in equations 10–12 [49], which can affect H_2O_2 amounts (equations 13–14). The Scavenging of the hydroxyl radicals by chloride results in the creation of active chlorine reactive species (Cl· (E_0=2.4 V) and $Cl_2\cdot$- (E_0=2.0 V)) that can efficiently react with many organic compounds. Cycling between chloride, chlorine, chlorine radicals, and dichlorine radicals can have an impact on PCT degradation (equations 14–19).

$$2Cl^- \rightarrow 2e^- + Cl_2 \tag{10}$$

$$Cl_2 + H_2O \rightarrow HOCl + Cl^- + H^+ \tag{11}$$

$$Cl_2 + H_2O_2 \rightarrow 2H^+ + O_2 + 2Cl^- \tag{12}$$

$$ClO^- + H_2O_2 \rightarrow H_2O + O_2 + Cl^- \tag{13}$$

$$Cl^- + HO\cdot \rightarrow Cl\cdot + OH^- \tag{14}$$

$$HO\cdot + Cl^- \rightarrow ClOH^- \quad k = 4.3 \times 10^9 \ M^{-1} \ s^{-1} \tag{15}$$

$$Cl^- + Cl\cdot \rightarrow Cl_2^- \quad k = 2.1 \times 10^{10} \ M^{-1} \ s^{-1} \tag{16}$$

$$Cl_2^- + Cl_2^- \rightarrow Cl_2 + 2Cl^- \quad k = 6.3 \times 10^8 \ M^{-1} \ s^{-1} \tag{17}$$

$$Cl_2^- + Cl\cdot \rightarrow Cl_2 + Cl^- \quad k = 2.1 \times 10^9 \ M^{-1} \ s^{-1} \tag{18}$$

$$Cl\cdot + Cl\cdot \rightarrow Cl_2 \quad k = 8.8 \times 10^7 \ M^{-1} \ s^{-1} \tag{19}$$

Model Fitting and Validation
Analysis of variance (ANOVA) was used to determine the model's significance, the statistically significant factors, and
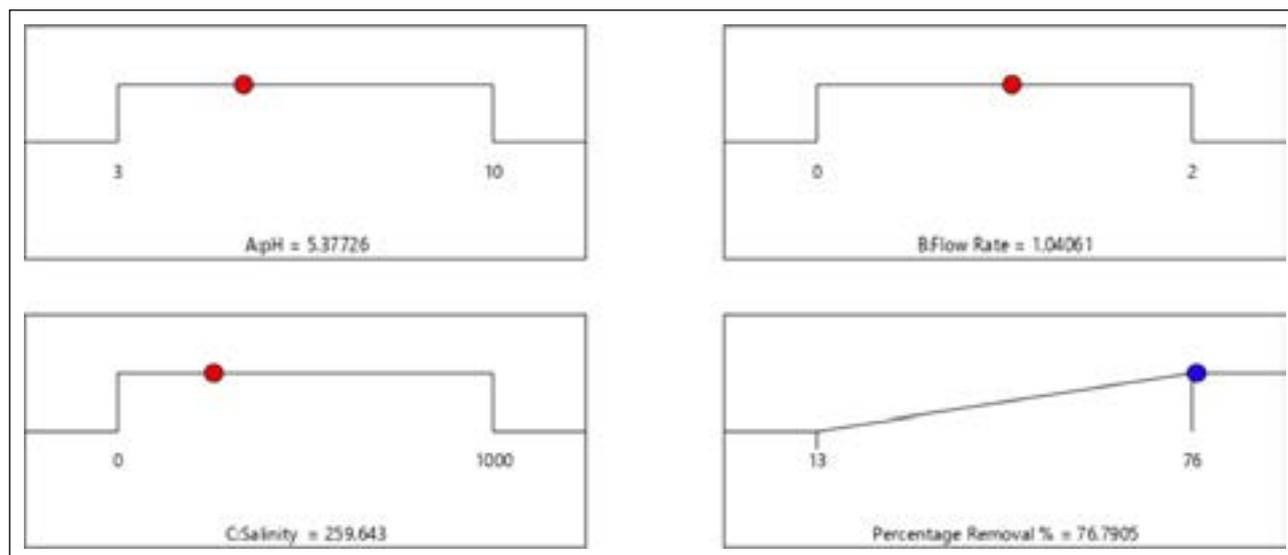
Figure 6. The optimization results.

appropriateness. The predicted and adjusted R^2 values were used to select the best model for the computational study as shown in Table 3. The best model—second-order polynomial regression was chosen for its highest values of R^2. The response of COD removal% is related to the input factors via the following equation.

$$R\% = = -33.2 + 31.6A + 32.3B + 0.021C + 0.878AB + 0.0014AC - 0.007BC - 2.77A^2 - 20.37B^2 - 0.000023C^2 \qquad (20)$$

The experimental values vs. the predicted values of % COD removal obtained by the RSM model are shown in Figure 5. This is the most crucial graph in the diagnostic instrument. It enables the detection of a value or set of values that cannot be easily anticipated by the model. The 45-degree line should divide the data points evenly. In this model, the points are fairly near the diagonal line. The little discrepancy between actual and anticipated values demonstrates a high connection between them. The results reveal that the experimental values and the quadratic model correspond well.

Table 4 shows the performance of the ANOVA test of the predicted model. The p-value is the ANOVA coefficient used to assess the significance of the source to the response in the quadratic regression, with a p-value of less than 0.05 being statistically significant. In general, there are three categories of terms: first order (A, B, and C), two-way interaction (AB, AC, and BC), and pure quadratic (A^2, B^2, and C^2). According to the analytical results in Table 4, the linear terms A and B are significant, with p-values of 0.0013 and 0.013, respectively. The pure quadratic terms A and B are also significant terms. The quadratic term C is likewise important, although it has a lower p-value of 0.067. The table shows that the interaction terms have a higher p-value (>0.05, terms that were not statistically significant). Based on the F-values of the variables, the order of factors that impact the effectiveness of removal is as follows: pH (A), air flow rate (B), and salinity(C).
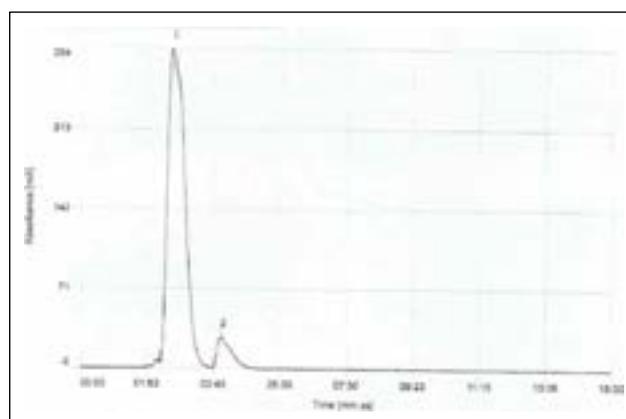
Figure 7. HPLC analysis of the treated sample (after 240 min. of photocatalysis).

The Optimization Result

The primary objective of the RSM study is to establish the optimal values of the variables to get the maximum value of paracetamol degradation based on experimental data modeling. Numerical optimization using the models generated in the study explores the design space for factor configurations that fulfill the goals. The optimal condition is the one chosen based on attractiveness, as represented in the diagram below Figure 6 (pH 5.3, flow rate 1 L/ min, and salinity 259 mg/L) to get maximum removal efficiency 76.7%).

HPLC analysis

For quantitative analysis and estimation of the paracetamol concentration in the unknown sample, different concentrations of the standard substance (5, 10, 25, 50, and 100) ppm were prepared to draw the calibration curve through the straight-line equation shown. The equation of the straight line is shown by drawing between the concentration and area of the peak, and the equation is as follows:

$$\lambda = 0.0054 \, X + 2.4457 \qquad (21)$$

Table 5. A comparison with other references

Treatment method	Type of wastewater	Condition	Removal effectiveness	References
Electrocoagulation	Real wastewater	pH = 6, electrolyte concentration 2.0 gL^{-1}, and current density 272.72 Am^{-1}	TOC 66% COD 62 5%	[18]
Electrocoagulation	Synthetic wastewater	pH 4, interelectrode distance 2 cm, electrolyte concentration 1.5 gL^{-1} and current density 272.72 Am^{-1}	TOC 63.2% COD 60.8%	[18]
Oxidation of paracetamol by TiO_2/UV	Synthetic wastewater	0.1 g L-1 of TiO_2	90% of paracetamol in 160 minutes	[43]
Photocatalytic degradation using TiO_2 P25 and TiO_2/ cellulosic fiber	Synthetic wastewater	298 K, 0.4 g L^{-1}(TiO_2-P25), pH= 2.5–11.0 under UV light. TiO_2/cellulosic fiber mode combined with solar light	90% of 2.65×10^{-4}M paracetamol was degraded under UV irradiation.	[42]
Photo-Fenton	Synthetic wastewater	hydrogen peroxide (H_2O_2) activation with a copper-based metal-organic	95% of paracetamol was degraded in 60 min.	[50]
Photocatalysis	Synthetic wastewater	photocatalyst consisting of titanium dioxide (TiO_2) and activated carbon (AC)	95% of the Paracetamol photodegradation	[51]
Photocatalysis	Synthetic wastewater	experiments were conducted at pH=7, Flow rate 1 L/min	COD 78%, and 91.2% of paracetamol was degraded	Present study

Where λ represents the concentration value and X represents the peak area.

The analysis of HPLC Analysis done for the solution test with 300 ppm of paracetamol concentration treated at the best condition, which gives higher values of COD removal efficiency, pH 7, flow rate 1L/min, and UV irradiation time 240 minutes. The chromatogram of paracetamol after treatment is shown in Figure 7. The paracetamol standard peak was shown after 2.3 min with the area of the peak of 4435.3 and this represents 26.4 ppm of paracetamol concentration. Hence, at these operating conditions, it may be presumed that complete degradation of paracetamol (91.2%) was observed. Comparing this result with other workers, the obtained results are in agreement with other workers, as shown in Table 4.

CONCLUSIONS

Photocatalysts process aided with air bubbles and UV light was applied to assess the degradation of paracetamol via the COD test and HPLC analysis under different operating conditions of pH, flow rate, and salinity. Surface Response methodology was used to predict the operating values as well as the optimum conditions. The results show that the COD removal percentage was well predicted by the quadratic equation calculated statistically by the Box-Benhken method indicated by the R^2 value (0.938). The results show that all three factors could affect pollutant adsorption on the photocatalyst surface. The effect of pH is partially attributed to its influence on pollutant adsorption on the photocatalyst surface and the electrostatic repulsion between the TiO_2 surface and paracetamol. Indeed, the results show that greater removal efficiency of COD occurs with the presence of air bubbles at 1 L/min. This is caused by two reasons, the

first enhancing the diffusion and mobility of Paracetamol molecules towards the active sites of the catalyst. The second is enhancing the generation of active (·OH). The salinity of the solution showed little significant prohibiting effect compared with the other two variables. Moreover, the p-values predicted by the Box- Benhken method showed that the single and quadratic terms of the variables have a significant effect. However, the effect between the variables (AB, AC, and BC) is negligible. According to the numerical optimization, the maximum % COD removal is 76.7 in the process conditions of 5.3 pH, 1 L/min, and 269 mg/L of NaCl. The experimental results show that the maximum % COD removal was 78% at pH=7, 1 L/min, and 0 mg/L of NaCl. The highest paracetamol degradation was 91.2% using HPLC analysis when pH=7 and flow rate 1 L/min and after 240 minutes.

DATA AVAILABILITY STATEMENT

The author confirm that the data that supports the findings of this study are available within the article. Raw data that support the finding of this study are available from the corresponding author, upon reasonable request.

CONFLICT OF INTEREST

The author declared no potential conflicts of interest with respect to the research, authorship, and/or publication of this article.

ETHICS

There are no ethical issues with the publication of this manuscript.

REFERENCES

[1]   C. Gadipelly, A. Pérez-González, G. D. Yadav, I. Ortiz, R. Ibáñez, V. K. Rathod, and K. V. Marathe, "Pharmaceutical industry wastewater: Review of the technologies for water treatment and reuse," Industrial & Engineering Chemistry Research, Vol. 53(29), pp. 11571–11592, 2018. [CrossRef]

[2]   A. R. Ribeiro, O. C. Nunes, M. F. R. Pereira, and A. M. T. Silva, "An overview of the advanced oxidation processes applied for the treatment of water pollutants defined in the recently launched directive 2013/39/EU," Environment International, Vol. 75, pp. 33–51. [CrossRef]

[3]   T. Heberer, "Tracking Persistent Pharmaceutical Residues from Municipal Sewage to Drinking Water," Journal of Hydrology, Vol. 266(3–4), pp. 175–189, 2002. [CrossRef]

[4]   C. Tixier, H. P. Singer, S. Oellers, and S. R. Müller, "Occurrence and fate of carbamazepine, clofibric acid, diclofenac, ibuprofen, ketoprofen, and naproxen in surface waters," Environmental Science & Technology, Vol. 37(6), pp. 1061–1068, 2003. [CrossRef]

[5]   K. Fent, A. A. Weston, and D. Caminada, "Ecotoxicology of human pharmaceuticals," Aquatic Toxicology, Vol. 76(2), pp. 122–159, 2006. [CrossRef]

[6]   C. Miège, J. M. Choubert, L. Ribeiro, M. Eusèbe, and M. Coquery, "Fate of pharmaceuticals and personal care products in wastewater treatment plants—conception of a database and first results," Environmental Pollution, 157(5), pp. 1721–1726, 2008. [CrossRef]

[7]   K. Kümmerer, "The presence of pharmaceuticals in the environment due to human use-present knowledge and future challenges," Journal of Environmental Management, Vol. 90(8), pp. 2354–2366, 2009. [CrossRef]

[8]   S. Mompelat, B. Le Bot, and O. Thomas, "Occurrence and fate of pharmaceutical products and by-products, from resource to drinking water," Environment International, Vol. 35(5), pp. 803–814, 2009. [CrossRef]

[9]   I. M. Sebastine, and R. J. Wakeman, "Consumption and environmental hazards of pharmaceutical substances in the UK," Process Safety Environmental Protection, Vol. 81(B4), pp. 229–235, 2003. [CrossRef]

[10]   L. Yang, L. E. Yu, and M. B. Ray, "Degradation of paracetamol in aqueous solutions by TiO2 photocatalysis," Water Research, Vol. 42(13), pp. 3480–3488, 2008. [CrossRef]

[11]   B. C. Lourenção, R. A. Medeiros, R. C. Rocha-Filho, L. H. Mazo, and O. Fatibello-Filho, "Simultaneous voltammetric determination of paracetamol and caffeine in pharmaceutical formulations using a boron-doped diamond electrode," Talanta, Vol. 78(3), pp. 748–752, 2009. [CrossRef]

[12]   M. Solé, J. P. Shaw, P. E. Frickers, J. W. Readman, and T. H. Hutchinson, "Effects on feeding rate and biomarker responses of marine mussels experimentally exposed to propranolol and acetaminophen," Analytical and Bioanalytical Chemistry, Vol. 96, pp. 649–656, 2010. [CrossRef]

[13]   K. H. Langford, and K. V. Thomas, "Determination of pharmaceutical compounds in hospital effluents and their contribution to wastewater treatment works," Environment International, Vol. 35(5), pp. 766–770, 2009. [CrossRef]

[14]   P. J. Phillips, S. G. Smith, D. W. Kolpin, S. D. Zaugg, H. T. Buxton, E. T. Furlong, K. Esposito, and B. Stinson, "Pharmaceutical formulation facilities as sources of opioids and other pharmaceuticals to wastewater treatment plant effluents," Environmental Science & Technology, Vol. 44(13), pp. 4910–4916, 2010. [CrossRef]

[15]   J. J. Xu, B. S. Hendriks, J. Zhao, and D. Graaf, "Multiple effects of acetaminophen and p38 inhibitors: towards pathway toxicology," FEBS Letters, Vol. 582, pp. 1276–1282, 2008. [CrossRef]

[16]   A. Carabin, P. Drogui, and D. Robert, "Photo-degradation of carbamazepine using TiO2 suspended photocatalysts," Journal of Taiwan Institute of Chemical Engineers, Vol. 54, pp. 109–117. [CrossRef]

[17]   N. Muir, J. D. Nichols, M. R. Stillings, and J. Sykes, "Comparative bioavailability of aspirin and paracetamol following single dose administration of soluble and plain tablets," Current Medical Research Opinion, Vol. 13(9), pp. 491–500, 1997. [CrossRef]

[18]   J. Wang, and S. Wang, "Removal of pharmaceuticals and personal care products (PPCPs) from wastewater: a review," Journal of Environmental Management, Vol. 182, pp. 620–640, 2016. [CrossRef]

[19]   M. Chen, F. Zhang, C. Cui, X. Liao, J. Chen, J. Rong, and D. Yu, "Treatment of wastewater from paracetamol factory by using non-thermal plasma and active carbon," 2011 International Conference on Materials for Renewable Energy & Environment, 2011. [CrossRef]

[20]   U. Nielsen, C. Hastrup, M. M. Klausen, B. M. Pedersen, G. H. Kristensen, J. L. C. Jansen, S. N. Bak, and J. Tuerk, "Removal of APIs and bacteria from hospital wastewater by MBR plus O3, O3 + H2O2, PAC or ClO2," Water Science and Technology, Vol. 67, pp. 854–862, 2013. [CrossRef]

[21]   M. Mameri, N. Debbache, M. E. M. Benacherine, N. Seraghni, and T. Sehili, "Heterogeneous photodegradation of paracetamol using Goethite/H2O2 and Goethite/oxalic acid systems under artificial and natural light," Journal of Photochemistry and Photobiology A: Chemistry, Vol. 315, pp. 129–137, 2016. [CrossRef]

[22]   M. E. M. Benacherine, N. Debbache, I. Ghoul, and Y. Mameri, "Heterogeneous photoinduced degradation of amoxicillin by Goethite under artificial and natural irradiation," Journal of Photochemistry and Photobiology A: Chemistry, Vol. 335, pp. 70–77, 2017. [CrossRef]

[23]   H. Al Qarni, P. Collier, J. O'Keeffe, and J. Akunna, "Investigating the removal of some pharmaceutical compounds in hospital wastewater treatment plants operating in Saudi Arabia," Environmental Science and Pollution Research, Vol. 23, pp. 13003–11301, 2016. [CrossRef]

[24] F. G. Dalgic, I. Turkdogan, K. Yetilmezsoy, and E. Kocak, "Treatment of real paracetamol wastewater by fenton process," Chemical Industry and Chemical Engineering, Vol. 23, pp. 23–29. [CrossRef]

[25] C. M. Lee, P. Palaniandy, N. Q. Zaman, and M. N. Adlan, "Pharmaceutical removal from synthetic wastewater using heterogeneous – photocatalyst," Applied Mechanics and Materials, Vol. 802, Article 507, 2015. [CrossRef]

[26] J. P. Scott, and D. F. Ollis, "Integration of chemical and biological oxidation processes for water treatment," Environ. Program, Vol. 14, pp. 88–103, 1995. [CrossRef]

[27] I. K. Konstantinou, and T. A. Albanis, "TiO2-assisted photocatalytic degradation of azo dyes in aqueous solution: kinetic and mechanistic investigations – a review," Applied Catalysis B: Environmental, Vol. 49, pp. 1–14, 2004. [CrossRef]

[28] M. A. Al-Nuaim, A. A. Al-Wasiti, Z. Y. Shnain, and A. K. AL-Shalal, "The combined effect of bubble and photo catalysis technology in btex removal from produced water," https://ejournal.undip.ac.id/ Accessed on Nov 02, 2023. [CrossRef]

[29] N. E. Mousa, S. S. Mohammed, Z. Y. Shnain, M. F. Abid, A. A. Alwasiti, and K. A. Sukkar, "Catalytic photodegradation of cyclic sulfur compounds in a model fuel using a bench-scale falling-film reactor ırradiated by a visible light," Bulletin of Chemical Reaction Engineering & Catalysis, Vol. 17(4), pp. 755–767, 2022. [CrossRef]

[30] H. Shemer, Y. K. Kunukcu, and K. G. Linden, "Degradation of the pharmaceutical metronidazole via UV, Fenton and photo-Fenton processes," Chemosphere, Vol. 63, pp. 269–276, 2005. [CrossRef]

[31] S. A. Abdulrahman, S. S. Ibraheem, and Z. Y. Shnain, "An overview of wastewater treatment using combined heterogeneous photocatalysis and membrane distillation," Chimica Techno Acta, Vol. 10(1), Article 10114, 2023. [CrossRef]

[32] A. K. Majhool, K. A. Sukkar, and M. A. Alsaffar, "Combining α-Al2O3 packing material and a ZnO nanocatalyst in an ozonized bubble column reactor to ıncrease the phenol degradation from wastewater," Processes, Vol. 11, Article 2416, 2023. [CrossRef]

[33] Y. Cheng, H. Sun, W. Jin, and N. Xu, "Photocatalytic degradation of 4-chlorophenol with combustion synthesized TiO2 under visible light irradiation," Chemical Engineering Journal, Vol. 128, pp. 127–133, 2007. [CrossRef]

[34] S. A. Abdulrahman, Z. Y. Shnain, S. S. Ibrahim, and H. S. Majdi, "Photocatalytic degradation of ciprofloxacin by uv light using n-doped tio2 in suspension and coated forms," Catalysts, Vol. 12, Article 1663, 2022. [CrossRef]

[35] F. S. Freyria, M. Armandi, M. Compagnoni, G. Ramis, I. Rossetti, and B. Bonelli, "Catalytic and photocatalytic processes for the abatement of n-containing pollutants from wastewater. part 2: Organic pollutants," Journal of Nanoscience and Nanotechnology, Vol. 17, pp. 3654–3672, 2017. [CrossRef]

[36] M. Compagnoni, G. Ramis, F. S. Freyria, M. Armandi, B. Bonelli, and I. Rossetti, "Photocatalytic processes for the abatement of n-containing pollutants from wastewater. Part 1: Inorganic pollutants," Journal of Nanoscience and Nanotechnology, Vol. 17(6), pp. 3632–3653, 2017. [CrossRef]

[37] N. Blangetti, F. S. Freyria, M. C. Calviello, N. Ditaranto, S. Guastella, and B. Bonelli, "Photocatalytic degradation of paracetamol under simulated sunlight by four TiO2 commercial powders: An insight into the performance of two sub-micrometric anatase and rutile powders and a nanometric brookite powder," Catalysts, Vol. 13(2), Article 434, 2023. [CrossRef]

[38] M.A. Al-Nuaim, A.A. Alwasiti, and Z.Y. Shnain, "The photocatalytic process in the treatment of polluted water," Chemical Papers, Vol. 77, pp. 677–701, 2023. [CrossRef]

[39] K.-H. Wang, Y.-H. Hsieh, C.-H. Wu, and C.-Y. Chang, "The pH and anion effects on the heterogeneous photocatalytic degradation of o-methylbenzoic acid in TiO2 aqueous suspension," Chemosphere, Vol. 40(4), pp. 389–394, 2000. [CrossRef]

[40] H.Y. Chen, O. Zahraa, and M. Bouchy, "Inhibition of the adsorption and photocatalytic degradation of an organic contaminant in an aqueous suspension of TiO2 by inorganic ions," Journal of Photochemistry and Photobiology A: Chemistry, Vol. 108(1), pp. 37–44, 1997. [CrossRef]

[41] J. P. Holmberg, E. Ahlberg, J. Bergenholtz, M. Hassellöv, and Z. Abbas, "Surface charge and interfacial potential of titanium dioxide nanoparticles: Experimental and theoretical investigations," Journal of Colloid Interface Science, Vol. 407, pp. 168–176, 2013. [CrossRef]

[42] N. Jallouli, K. Elghniji, H. Trabelsi, and M. Ksibi, "Photocatalytic degradation of paracetamol on TiO2 nanoparticles and TiO2/cellulosic fiber under UV and sunlight irradiation," Arabian Journal of Chemistry, Vol. 10(Suppl 2), pp. S3640–S3645. [CrossRef]

[43] T. M. A. Dalmázio, R. Alves, and R. Augusti, "An appraisal on the degradation of paracetamol by TiO2/ UV system in aqueous medium. Product identification by gas chromatography–mass spectrometry," Journal of the Brazilian Chemical Society, Vol. 19(1), pp. 81–88, 2008. [CrossRef]

[44] A. Sclafani, L. Palmisano, and E. Davi, "Photocatalytic degradation of hydroxyethylcellulose in aqueous Pt TiO2 suspension," Journal of Photochemistry and Photobiology A: Chemistry, Vol. 56, pp. 399–406, 1991. [CrossRef]

[45] M. Fujihira, Y. Satoh, and T. Osa, "Photocatalytic degradation of organic water contaminants: Mechanisms involving hydroxyl radical attack," Bull Chem Soc 1982. [CrossRef]

[46] C. Kormann, D.W. Bahnemann, and M. R. Hoffmann, "Photolysis of chloroform and other organic molecules in aqueous titanium dioxide suspensions," Environmental Science & Technology, Vol. 25, pp. 494–500, 1991. [CrossRef]

[47] D. F. Ollis, C. Y. Hsiar, L. Budiman, and C. L. Lee, "Visible-light activation of TiO2 photocatalysts: Advances in theory and experiments," Journal of Photochemistry and Photobiology C: Photochemistry Reviews, Vol. 25, pp. 1–29, 2015. [CrossRef]

[48] C. Maillard-Dupuy, C. Guillard, and P. Pichat, "Kinetics and products of the TiO2 photocatalytic degradation of pyridine in water," Environmental Science & Technology, Vol. 28, pp. 2176–2183, 1994. [CrossRef]

[49] E. Mostafa, P. Reinsberg, S. Garcia-Segura, and H. Baltruschat, "Chlorine species evolution during electrochlorination on boron-doped diamond anodes: In-situ electrogeneration of Cl2, Cl2O and ClO2," Electrochimica Acta, Vol. 281, pp. 831–840, 2018. [CrossRef]

[50] A. Abdelhaleem, H. N. Abdelhamid, M. G. Ibrahim, and W. Chu, "Photocatalytic degradation of paracetamol using photo-Fenton-like metal-organic framework-derived CuO@C under visible LED," Journal of Cleaner Production, Vol. 379, Article 134571, 2022. [CrossRef]

[51] D. C. Sanches Gloria, C. H. Vieira Brito, T. A. Prado Mendonça, T. R. Brazil, R. A. Domingues, N. C. Silva Vieira, E. B. Santos, and M. Gonçalves. "Preparation of TiO2/activated carbon nanomaterials with enhanced photocatalytic activity in paracetamol degradation," Materials Chemistry and Physics, Vol. 305, Article 127947, 2023. [CrossRef]